Electric field effect in ligand electron–nuclear double resonance of cubic centers in a CaF_2:Gd^{3+} crystal

S. M. Arkhipov, N. V. Legkikh, B. Z. Malkin, and Yu. A. Sherstkov

*A. M. Gorkiĭ Urals State University, Sverdlovsk
and V. I. Ulyanov-Lenin State University, Kazan*
(Submitted 16 September 1977; resubmitted 10 December 1977)
Zh. Eksp. Teor. Fiz. **74**, 1717–1726 (May 1978)

The linear electric field effect in the ENDOR spectra of fluorine ions in the first coordination sphere of Gd^{3+} impurities in the fluorite lattice was investigated at liquid helium temperature in fields up to 600 kV/cm. The parameters of the effective Hamiltonian of the superhyperfine interactions in an electric field were found from the orientational dependence of the pseudo-Stark splittings of the ENDOR lines. The published data on changes in the ENDOR spectra under the influence of uniaxial and hydrostatic pressures and the results of a microscopic calculation of local structure of the impurity lattice were used to determine the contributions of the various mechanisms to the electric field effect. It was found that the electric polarization of ions played the dominant role in the change in the isotropic superhyperfine interaction constant.

PACS numbers: 76.70.Dx

INTRODUCTION

A study of the spectra of paramagnetic centers in an external electric field is one of the essential elements in a comprehensive investigation of activated crystals. The information on the local structure and electric polarization of the impurity lattice deduced from the electric field effects is complementary to the data obtained from the Zeeman spectroscopic and piezospectroscopic studies.[1]

The symmetry relationships impose certain restrictions on the possibility of observing the electric field effect; in the case of impurity centers of the cubic symmetry the linear (in respect of the electric field) changes in the energy spectrum are possible only for neighbors of a defective lattice site whose point symmetry group does not include the inversion operation; in particular, there should be displacements and pseudo-Stark splittings of the NMR and ENDOR lines of ligands. Up to now the linear electric field effect in the ligand ENDOR has been determined only for the spectra of the F centers in alkali halide crystals.[2] The results of similar investigations of small-radius centers in crystals activated with transition ions have not yet been reported.

We determined the linear electric field effect in the ENDOR spectra of the nuclei of the F^- ions in the first coordination sphere of substitutional impurity centers (Gd^{3+} ions) in fluorite. The ligand ENDOR spectra of crystals with the fluorite structure activated with rare-earth ions are used widely in investigations of the mechanisms of the superhyperfine interaction and local structure of the impurity centers. An analysis of the experimental data on the ENDOR spectra of a CaF_2:Gd^{3+} crystal under hydrostatic[3] and uniaxial[4] pressures, based on a microscopic calculation of the spatial structure of the impurity lattice, enabled us to obtain preliminary estimates of the magnitude of the electric field effect. Measurements of the orientational dependence of this effect yielded the parameters of the effective superhyperfine interaction Hamiltonian in an external electric field; we determined that the contributions made to the

superhyperfine interaction parameters by the change in the length and direction of the radius vector of the fluorine ion in an electric field, and by the polarizations of the fluorine and gadolinium ions. Measurements of the electric field effect confirmed the Baker hypothesis[5] of the important role of the electron polarization in the formation of the magnetic field at the nuclei of paramagnetic ion ligands.

EXPERIMENTAL METHOD AND RESULTS

The experiments were carried out at liquid helium temperature with a 3-cm superheterodyne ESR spectrometer[6] fitted with an additional rf source. The six-turn rf coil consisted of two rows of copper wires which passed through the narrow walls of a microwave resonator; the distance between the two rows was 9 mm and the distance between wires in each row was 1.5 mm. An internally silvered ceramic resonator (for the H_{102} mode) had a Q factor of ~3000 when loaded with a sample. The sample was placed at the center of the resonator and rf coil on a rotating polystyrene holder. The ability to rotate the magnet and holder independently about mutually perpendicular axes made it possible to orient the sample with sufficient accuracy in the determination of angular dependences of the spectra.

The spectrometer was tuned to the imaginary part of the electronic susceptibility. The klystron frequency was stabilized by an AFC system using a signal resonator. The ENDOR signals were recorded under conditions of frequency or amplitude modulation of the rf oscillations (the modulation frequency was ν_m ~ 400 Hz). The resonance conditions were not modulated in the ESR case. It was found that the optimal conditions in the ENDOR line recording were provided by a microwave power of 25–30 dB (measured from 100 mW) and an rf magnetic field amplitude of ~0.5 G.

The samples were prepared from fluorite single crystals with a Gd^{3+} ion concentration of 0.05 wt.% in the charge, grown by the Stockbarger method in a helium
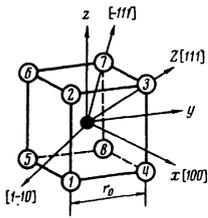
0038-5646/78/050896-06$02.40

FIG. 1. Immediate environment of cations in the fluorite lattice. $\bigcirc$)F$^-$; $\bullet$) Ca^{2+} (Gd^{3+}).

atmosphere. These samples were oriented plates 0.35 mm thick with evaporated metal electrodes to which Teflon-insulated wire electrodes were soldered. A sample was embedded in a silicone adhesive containing a filler. Fields of up to 600 kV/cm intensity were applied in measurements of the electric field effect. The ENDOR spectra of the investigated samples included lines of the tetragonal fluorine and cubic Gd^{3+} centers. The electric field effect was observed in both types of spectra; in the present paper we shall report only the results obtained for the spectra of the cubic centers (with a nonlocal compensation of the excess charge of the Gd^{3+} impurity ions, occupying the Ca^{2+} cation sites: see Fig. 1).

In a static homogeneous electric field E the ENDOR frequencies of the cubic centers, representing transitions between energy levels of the nucleus (spin $I=\frac{1}{2}$) of a fixed ligand, are governed by the eigenvalues of the Hamiltonian $\mathcal{H}$, which has the simplest form in a local coordinate system X, Y, Z with the Z axis along the symmetry axis of a given ligand (see Fig. 1):

$$\mathcal{H}/h = v_z Se + v_L Ie + (A_\parallel + V_\parallel E_z) I_z S_z$$
$$+ (A_\perp + V_\perp E_z)(I_x S_x + I_y S_y) + V[E_x(I_z S_x + I_x S_z)$$
$$+ E_Y(I_z S_Y + I_y S_z)] \ldots ; \tag{1}$$

here, e is a unit vector in the direction of a static magnetic field H; v_z and v_L are the frequencies of the Larmor precession of, respectively, the rare-earth ion with an effective spin S and the ligand nucleus;

$$A_\parallel = A_s + 2A_p, \quad A_\perp = A_s - A_p, \tag{2}$$

where A_s and A_p are the isotropic and anisotropic superhyperfine interaction constants; independent components of the third-rank tensor $V_{\alpha\beta\gamma}$ ($V_{ZZZ} = V_\parallel$, $V_{ZXX} = V_\perp$, $V_{XXZ} \doteq V_{XZX} = V)^{[1]}$ govern the changes in the superhyperfine interaction tensor in the electric field; the terms nonlinear in respect of the components of the spin moment of the paramagnetic ion are omitted from Eq. (1).

In a strong magnetic field ($v_z \gg A_s, A_p$) the ENDOR frequencies in the rare-earth ion state with a projection of the spin M on the field H making an angle θ with the Z axis are

$$v(M) = v_0(M) + \Delta v(M), \tag{3}$$

where

$$v_0^2(M) = [v_L + MA_s + MA_p(3\cos^2\theta - 1)]^2 + (^3/_2 MA_p \sin 2\theta)^2, \tag{4}$$

and the frequency shift linear in respect of the electric

field is given by

$$\Delta v(M) = \frac{M}{v_0(M)} \left\{ \left[\left(v_0^2(M) \right. \right. \right.$$
$$\left. - \left(\frac{3}{2} MA_p \sin 2\theta \right)^2 \right)^{1/2} \left(\frac{\partial A_s}{\partial E_z} \right.$$
$$\mp (3\cos^2\theta - 1) \frac{\partial A_p}{\partial E_z} \right) + \left(\frac{3}{2} \sin 2\theta \right)^2 MA_p \frac{\partial A_p}{\partial E_z} \right] E_z$$
$$\left. - \frac{1}{2} \sin 2\theta \cos(\varphi - \varphi_E) [2v_L + M(2A_s + A_p)] VE_\perp \right\}. \tag{5}$$

Here, $E_\perp = E\sin\theta_E$ is the component of the field E perpendicular to the bond axis; $\varphi - \varphi_E$ is the angle between the projections of the vectors H and E on the XY plane;

$$\frac{\partial A_s}{\partial E_z} = \frac{1}{3}(V_\parallel + 2V_\perp), \quad \frac{\partial A_p}{\partial E_z} = \frac{1}{3}(V_\parallel - V_\perp). \tag{6}$$

Any line in the ENDOR spectrum of the cubic centers of frequency $v_0(M)$ represents at least a sum of signals from two ligands linked by the inversion operation. In the electric field these ions become magnetically equivalent, the corresponding signals shift by $\pm|\Delta v(M)|$, and the ENDOR lines experience pseudo-Stark splitting by an amount $\Delta = 2|\Delta v(M)|$.

The results of the measurements of Δ for the $\frac{1}{2} \longleftrightarrow -\frac{1}{2}$ electronic transition are listed in Table I for various orientations of the magnetic and electric fields relative to the tetragonal crystallographic coordinate system (Fig. 1). The measured ENDOR frequencies $v_0(M)$, also included in Table I, are described satisfactorily by Eq. (4) if we choose the published$^{[7]}$ values of A_s and A_p (see Table II). A significant electric field effect is observed for the ENDOR signals of the nuclei in the first coordinate sphere (Fig. 2) in those cases when the electric field is directed along the trigonal symmetry axis of the lattice and the effect is maximal in $E \perp H$ for signals of the ligands with the bond axis parallel to the electric field.

The magnitudes of the pseudo-Stark splittings Δ_n in Table I are described, within the indicated limits of the experimental error, by Eq. (5) if we adopt the following characteristics of the electric field effect: $|V_\parallel| \leqslant 3$, $|V_\perp| = 63 \mp 1$, $|V| = 56 \mp 3$ Hz/(kV/cm), where $V_\parallel$, $V_\perp$, and V should have the same signs.

On the basis of the results obtained we may expect a considerable electric field effect in parallel E and H

TABLE I. Pseudo-Stark splittings in ENDOR spectrum of ligand nuclei in CaF$_2$:Gd^{3+} crystal subjected to electric field $E = 500$ kV/cm.

n	Field directions		Ligands	v_L, MHz	M	$v_0(M)$, MHz	Δ_n, kHz
---	H	E					
1	[1 0 0]	[0 1 0]	1–8	13.00	$-^1/_2$	14.40	<3
2	[1 −1 0]	[1 1 1]	3.5	12.83	$-^1/_2$	16.25	30±2
3	[1 −1 0]	[1 1 1]	4.6	12.83	$-^1/_2$	16.25	<10
4	[1 1 1]	[1 1 1]	3.5	13.174	$+^1/_2$	17.47	<3
5	[1 1 1]	[−1 1 1]	3.5	13.174	$+^1/_2$	17.47	<3
6	[1 1 1]	[−1 1 1]	1.7	13.174	$-^1/_2$	16.00	30±2
7	[1 1 1]	[−1 1 1]	2.4.6.8	13.174	$-^1/_2$	16.00	<5
8	[1 1 1]	[1 1 1]	1.2.4 6.7.8	13.174	$-^1/_2$	16.00	20±4

897   Sov. Phys. JETP 47(5), May 1978

Arkhipov et al.   897

TABLE II. Superhyperfine interaction constants of nuclei in first coordination sphere of Gd^{3+} ions in fluorite and their changes in external fields.

	$A = A_s$	$A = A_p$	Remarks
A, MHz	−1.89	5.09	According to Baker and Christidis[7]
$\dfrac{\Delta A}{p}$, $\dfrac{kHz}{kG/mm^2}$	−0.064∓0.057	0.434∓0.02	According to Kasatochkin and Yakovlev[3]; hydrostatic pressure
$\dfrac{\Delta A}{P_{[111]}}$, $\dfrac{kHz}{kG/mm^2}$	−0.63	0.72	According to Baker and Christidis[4]; data for ligands on compression axis
$\dfrac{\partial A}{\partial E_z}$, $\dfrac{Hz}{kV/cm}$	∓43±1	±20±1	Upper and lower signs refer to nuclei with radius vectors parallel and antiparallel to E
$\dfrac{\partial A}{\partial R}$, $\dfrac{MHz}{\text{Å}}$	0.1±1.2	−7.69	−
$\dfrac{\partial A}{\partial D_z(F)}$, $\dfrac{MHz}{e\text{Å}}$	−16.7±4.3	−8.17	−
$\dfrac{\partial A}{\partial D_z(Gd)}$, $\dfrac{MHz}{e\text{Å}}$	−12.8±2.6	2.82	−

oriented along the tetragonal lattice axis with $\Delta \sim 30$ kHz for the line investigated in the $n=1$ case. The doublet structure of this line, which is due to the indirect interaction of the magnetic moments of the ligands, is masked by the increasing (with the electric field) line width so that the pseudo-Stark splitting is not observed explicitly. An analysis of the nature of the broadening shows that the value of Δ in a field $E = 600$ kV/cm is at least 20 kHz.

DISCUSSION OF RESULTS

The interaction between the magnetic moments of the rare-earth ion and ligand nuclei is dominated by the direct dipole—dipole interaction and transfer of the electron spin density to the ligands because of the overlap of the ligand wave functions (in particular, the outer $2s$ and $2p$ functions of the F^- ions) with the $4f$ functions of the valence electrons[5,8] and with the $5s$ and $5p$ functions of the polarized filled rare-earth ion shells, dominating the formation of the magnetic field at the host nuclei of the ions in the S state.[9]

The changes in the superhyperfine interaction constants in an electric field are governed by the electronic and ionic polarizations of the lattice. The electronic polarization appears because of the mixing of the ground-

FIG. 2. Splitting of an ENDOR line in an electric field (see Table I, $n = 8$).

state configuration of an ion with its excited states. In calculating the spectrum of a nucleus of a fixed ligand we shall select the quantization axis to be the appropriate local Z axis and we shall write the one-electron wave functions of the polarized F^- and Gd^{3+} ions in the form

$$\psi_{\mu E} = \psi_\mu + \sum_\alpha E_\alpha \sum_{\mu'} \eta_{\mu\mu'}^\alpha \psi_{\mu'}, \qquad (7)$$

where

$$\eta_{\mu\mu'}^\alpha = e\langle\mu'|x_\alpha|\mu\rangle/(\varepsilon_{\mu'}-\varepsilon_\mu), \qquad (8)$$

x_α are the coordinates, $-e$ is the charge, and ε_μ are the energy levels of an electron; μ are the filled and μ' are the excited states of opposite parities.

The effective Hamiltonian of the superhyperfine interaction (1) is obtained by averaging the hyperfine interaction operator $\mathcal{H}_{hf}$[10] over the antibonding molecular orbitals of the complex $Gd^{3+}F_8^-$, constructed from the function (7), and by replacing in a suitable manner the one-electron spin operators with the total spin operator of the Gd^{3+} ion.

The contribution to Eq. (1) from the spin density transferred to a ligand is, to within terms linear in respect of the electric field components,

$$\sum_\mu \sum_{\rho\varkappa} \Big\{ S_{\mu\rho} S_{\mu\varkappa} \Big[\langle\rho|\mathcal{H}_{hf}|\varkappa\rangle + 2\sum_\alpha E_\alpha \sum_{\rho'} \eta_{\rho\rho'}^\alpha \langle\rho'|\mathcal{H}_{hf}|\varkappa\rangle \Big]$$
$$+ 2S_{\mu\varkappa} \sum_\alpha E_\alpha \Big[\sum_{\rho'} S_{\mu\rho'} \eta_{\rho\rho'}^\alpha \langle\rho|\mathcal{H}_{hf}|\varkappa\rangle$$
$$+ \sum_{\mu'} S_{\mu'\rho} \eta_{\mu\mu'}^\alpha \langle\rho|\mathcal{H}_{hf}|\varkappa\rangle \Big] \Big\} \lambda_{\mu\rho}\lambda_{\mu\varkappa}, \qquad (9)$$

where $\lambda_{\mu\rho} \geqslant 1$ are the coefficients of proportionality between the parameters of the covalent bond and overlap integrals

$$S_{\mu\rho}(E) = \langle\psi_{\mu E}(Gd)|\psi_{\rho E}(F)\rangle.$$

In particular, we shall consider the contributions made to the superhyperfine interaction constants by the $5s^2$ shell of the Gd^{3+} ion. If we assume that there is no electric polarization of the paramagnetic ion and ligands, allow for the dependences of the radial wave functions of the filled rare-earth ion shells (distinguished below by the signs "+" and "−") on the electron spin orientation parallel or antiparallel to the magnetic moment of the ion, and ignore the covalence of the bonds between the $5s$ electrons and the outer electron shells of the ligands ($\lambda_{5s,2s} = \lambda_{5s,2p\alpha} = 1$), we obtain[8,10]

$$A_s(5s) = \frac{1}{7}[\langle 5s^+|2s\rangle^2 - \langle 5s^-|2s\rangle^2]A_{2s},$$
$$A_p(5s) = \frac{1}{7}[\langle 5s^+|2pZ\rangle^2 - \langle 5s^-|2pZ\rangle^2]A_{2p}, \qquad (10)$$

where A_{2s} and A_{2p} are the characteristics of the hyperfine interaction of the F^- ion. We shall simplify the sums over the excited states by assuming that in the electric field the $2s$ function of the F^- ion is mixed only with the $3p$ functions, the $2p$ functions are mixed with the $3s$ function, and the $5s$ function of Gd^{3+} is mixed with
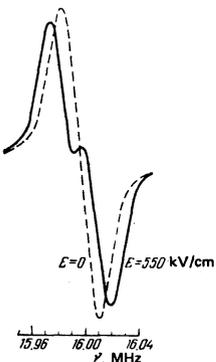
the $6p$ functions. Using Eq. (9), we obtain the following contributions of the $5s^2$ shell to the characteristics of the electric field effect

$$\frac{\partial A_s}{\partial E_z}(5s) = \frac{2}{7}A_{2s}\left[S_{5s,2s}\left(S_{5s,2pz}\eta_{2pz,3s}\frac{\psi_{3s}(0)}{\psi_{2s}(0)}\right.\right.$$
$$\left.\left.+S_{5s,3pz}\eta_{2s,3pz}+S_{6pz,2s}\eta_{5s,6pz}\right)\right]_-^+,\qquad(11)$$

$$\frac{\partial A_p}{\partial E_z}(5s) = \frac{2}{7}A_{2p}\left[S_{5s,2pz}\left(S_{5s,2s}\eta_{2s,3pz}\frac{\langle r^{-3}\rangle_{3p,2p}}{\langle r^{-3}\rangle_{2p,2p}}\right.\right.$$
$$\left.\left.+S_{5s,3s}\eta_{2pz,3s}+S_{6pz,2pz}\eta_{5s,6pz}\right)\right]_-^+,\qquad(12)$$

$$V(5s) = \frac{3}{7}A_{2p}\left[S_{5s,2pz}\left(S_{5s,2s}\eta_{2s,3px}\frac{\langle r^{-3}\rangle_{3p,2p}}{\langle r^{-3}\rangle_{2p,2p}}\right.\right.$$
$$\left.\left.+S_{5s,3s}\eta_{2px,3s}+S_{6px,2px}\eta_{5s,6px}\right)\right]_-^+,\qquad(13)$$

where $[B]_-^+ = B^+ - B^-$ is the difference between the quantities corresponding to different orientations of the $5s$- and $6p$-electron spins. The order-of-magnitude relationship is $\eta \sim (\alpha_0/\epsilon)^{1/2}$, where ϵ is the ionization energy and α_0 is the polarizability of an ion. The comparison of Eqs. (10) and (11)–(13) makes it possible to estimate the changes in the components of the superhyperfine interaction tensor due to the electric polarization; the order of magnitude is

$$V_{\alpha\beta\gamma} \sim A_s\left(\frac{\alpha_0}{\epsilon}\right)^{1/2}\frac{\langle 5s|3pZ\rangle}{\langle 5s|2s\rangle};$$

for $|A_s| = 2$ MHz, $\alpha_0 = 1$Å^3, $\epsilon = 10^5$ cm^{-1}, and allowance for the increase in the overlap integrals for the excited states by an order of magnitude shows that $|V_{\alpha\beta\gamma}| \sim 10$ Hz/(kV/cm), which is in agreement with the results of measurements of the electric field effect (see Table II).

The ionic polarization—representing displacements of the cation and anion sublattices relative to one another[11] —is responsible for changes in the orientation of the bond axes relative to the static magnetic field and for changes in the distances between the paramagnetic impurity ion and ligands. If we assume that the electric dipole moments $D(k)$ induced on the ions are proportional to the local electric field acting on them, we can use Eq. (9) to write the superhyperfine interaction parameter in the form $(A = A_s, A_p)$

$$A = A'(R) + \frac{\partial A}{\partial D_z(F)}D_z'(F),\qquad(14)$$

where R is the distance between the rare-earth ion and ligand; $D_z'(F)$ is the dipole moment of the ligand induced by the field of the excess charge of the impurity ion in the heterovalent substitution case. Under external forces acting on the lattice the changes in the components of the superhyperfine interaction tensor are

$$\Delta A = \frac{\partial A}{\partial R}\Delta R + \frac{\partial A}{\partial D_z(F)}D_z(F) + \frac{\partial A}{\partial D_z(Gd)}D_z(Gd),\qquad(15)$$

$$VE_\perp = V_\theta\frac{\partial\theta_\epsilon}{\partial E_\perp}E_\perp + V_{D(F)}D_\perp(F) + V_{D(Gd)}D_\perp(Gd),\qquad(16)$$

where ΔR is the change in the bond length; $D_z(k)$ and $D_\perp(k)$ are the longitudinal and perpendicular (to the bond axis) components of the dipole moment of the k-th ion induced by the external field. The quantity $V_\theta = -3A_p$ is found directly by comparing the derivative $\partial v_0(M)/\partial\theta$ of Eq. (4) with Eq. (5). The derivative $\partial A/\partial R$, $\partial A/\partial D_z(k)$ can be found using the ENDOR spectra of the ligands obtained under hydrostatic and uniaxial pressures.

According to Eq. (15), the application of a hydrostatic pressure p increases the superhyperfine interaction constants by the amounts ΔA_s and ΔA_p given by

$$\frac{\Delta A}{p} = -\frac{R}{c_{11}+2c_{12}}\left(\frac{e_1(\Gamma_{1g})}{e(\Gamma_{1g})}\frac{\partial A}{\partial R} + eD_1(\Gamma_{1g})\frac{\partial A}{\partial D_z(F)}\right);\qquad(17)$$

the application of pressure $p_{[111]}$ along the trigonal axis of the fluorite lattice produces the following increment in the case of the ligands on the compression axis (3 and 5 in Fig. 1):

$$\frac{\Delta A}{p_{[111]}} = \frac{1}{3}\left(\frac{\Delta A}{p}\right) - \frac{R}{6c_{44}}\left[\left(2\frac{e_1(\Gamma_{5g})}{e(\Gamma_{5g})} + W_1\right)\frac{\partial A}{\partial R} + eD_1\frac{\partial A}{\partial D_z(F)}\right],$$
$$\qquad(18)$$

where c_{ij} are the elastic constants of fluorite[12] and $e_1(\Gamma_{ig})/e(\Gamma_{ig})$ are the ratios transforming in accordance with irreducible representations Γ_{ig} of the group O_h of the strain tensor components of the first coordination shell of the rare-earth ion to the corresponding components of the strain tensor of the regular lattice. The dimensionless parameter $D_1(\Gamma_{1g})$ in Eq. (17) determines the dipole moments of the ligands induced by hydrostatic pressure; the parameters W_1 and D_1 in Eq. (18) are the characteristics of the displacement vectors and dipole moments of the ligands due to the microscopic deformation of the fluorite lattice (displacements and polarizations of the fluorine sublattices[13]), which appear together with microscopic strains under hydrostatic pressure $[e(\Gamma_{1g}) = -p_{[111]}/3(c_{11} + 2c_{12})]$ and shear caused by $p_{[111]}$ $[e_{\alpha\beta}(\Gamma_{5g}) = -p_{[111]}/6c_{44}, \alpha \neq \beta; \alpha,\beta = x, y, z]$.

In an external electric field $E\|[111]$ the changes in the superhyperfine interaction constants of the ligand 3 in Fig. 1 are [see Eq. (15)]

$$\frac{\partial A}{\partial E_z} = r_0(\Delta_\| + 2\Delta_\perp - \Delta_0)\frac{\partial A}{\partial R} + er_0D\frac{\partial A}{\partial D_z(Gd)}$$
$$+ er_0(D_\| + 2D_\perp)\frac{\partial A}{\partial D_z(F)}\qquad(19)$$

[for the ligand 5 the right-hand side of Eq. (19) has the opposite sign]. The dimensionless parameters introduced here specify the configuration of the $Gd^{3+}F_8^-$ complex and the ion polarization for an arbitrary orientation of the electric field. In particular, in a field $E\|z$ the cube shown in Fig. 1 is displaced against the field relative to the (assumed to be fixed) cation sublattice and transforms into a regular truncated tetrahedral pyramid[14]; the displacement vectors of the impurity ion (ΔR_0) and ligands (ΔR_i) are

$$\Delta R_0 = r_0\Delta_0 E,\qquad(20)$$

$$\Delta R_i = r_0(\Delta_\| - \Delta_\perp)E + r_0\Delta_\perp ER_i/z_i;\qquad(21)$$

the field-induced dipole moments of the ions are found by replacing in Eqs. (20) and (21) the quantities Δ_0, $\Delta_{||}$, $\Delta_\perp$ with D_0, $D_{||}$, $D_\perp$, respectively.

The structure and polarization of the fluorite lattice near the Gd^{3+} impurity ions, local elastic constants, and parameters of the cubic centers in an external electric field were calculated within the framework of the quasimolecular model[13-16] and the interactions between the ions were considered in the shell model[17]; the results of the calculations are given below.

a) The local deformation (strain) and polarization of the first coordination sphere:

$$\Delta R_z'(F) = \Delta' \cdot R, \quad D_z'(F) = eD' \cdot R,$$
$$\Delta' = 0.0353, \quad D' = 0.019 . \tag{22}$$

b) Hydrostatic compression:

$$e_1(\Gamma_{1g})/e(\Gamma_{1g}) = 0.663, \quad D_1(\Gamma_{1g}) = -0.0392. \tag{23}$$

c) Uniaxial compression (trigonal deformation)[1]:

$$e_1(\Gamma_{5g})/e(\Gamma_{5g}) = 0.776, \quad W_1 = -0.530 \ (-0.336), \quad D_1 = -0.324 \ (-0.292).$$

$$\tag{24}$$

d) Homogeneous electric field (the values are given in 10^{-10} cm/V):

$$\begin{aligned} \Delta_0 &= -3.54 \ (0.0), & D_0 &= 9.32 \ (7.29), \\ \Delta_{||} &= -14.90 \ (-16.06), & D_{||} &= 1.99 \ (2.07), \\ \Delta_\perp &= 1.28 \ (0.0), & D_\perp &= 0.11 \ (0.0). \end{aligned} \tag{25}$$

The substitution in Eqs. (17)-(19) of the data from (22)-(25) and of the results of measurements of $\Delta A/p$, $\Delta A/p_{[111]}$, $\partial A/\partial E_z$ give the derivatives $\partial A/\partial R$, $\partial A/\partial D_z(F)$, $\partial A/\partial D_z(Gd)$ listed in Table II. A comparison of the values of the various terms in Eq. (19) corresponding to the change (in the external fields) of the bond length and electrostatic polarization of the ligand and of the Gd^{3+} impurity ion

$$\partial A_s/\partial E_z = -0.2 - 10.1 - 31.7 \ \text{Hz/(kV/cm)},$$
$$\partial A_p/\partial E_z = 17.8 - 4.9 + 7.1 \ \text{Hz/(kV/cm)}$$

shows that the polarization (particularly that of the paramagnetic ion) plays the dominant role in the change in the isotropic superhyperfine interaction constant. The parameter V describing the influence of the component of the field E perpendicular to the bond axis is also governed mainly by the polarization of the Gd^{3+} ion and of the ligands: the contribution to the parameter V due to the tilting of the bond axis

$$V_\theta \partial \theta_E/\partial E_\perp = -2\sqrt{3} A_p (\Delta_\perp - \Delta_{||} + \Delta_0) \tag{26}$$

represents -39% of the measured value of V.

The contributions to the constants A_s and A_p due to the ligand polarizations are, in accordance with Eq. (14) and the results of calculations of the dipole moments $D_z'(F)$ induced on the F^- ions [see Eq. (22)], respectively $41 \pm 10\%$ of A_s and -7.5% of A_p.

If we use the known values of the superhyperfine in-

TABLE III. Superhyperfine interaction constants and structure parameters of $Cd^{3+}F_8^-$ complexes in MeF_2 crystals.

	CdF₂	SrF₂	BaF₂
ΔA_i, MHz [7]	0.11	0.00	0.56
ΔA_p, MHz [7]	0.07	-0.25	-0.47
ΔR_{00}, Å* [7]	-0.033	0.145	0.319
ΔR, Å [7]	-0.005	0.034	0.109
ΔR, Å	-0.0020∓0.0017	0.0318∓0.0026	0.1010∓0.002
$\Delta D_z'(F)$, eÅ	0.0019∓0.0069	0.0006∓0.0024	-0.035∓0.002
$\Delta D_z'(F)$, eÅ [16]		-0.016	-0.036

*Here, $\Delta R_{00} = \sqrt{3} \ [r_0(\text{MeF}_2) - r_0 \ (\text{CaF}_2)]/2$.

teraction constants of the homologous fluorite series,[7] we can apply two equations of the (15) type for ΔA_s and ΔA_p $[\Delta A = A(\text{MeF}_2) - A(\text{CaF}_2)]$ to find the changes in the radius of the first coordination sphere of the Gd^{3+} ion: $\Delta R = R(\text{MeF}_2) - R(\text{CaF}_2)$, as well as the dipole moments of the ligands: $\Delta D_z'(F) = D_z'(F)_{\text{MeF}_2} - D_z'(F)_{\text{CaF}_2}$. The results obtained (Table III) are close to the published estimates[17] and calculated results.[16]

Thus, a qualitative analysis of the influence of the external electric field on the wave functions of a paramagnetic center has enabled us to parametrize the changes in the superhyperfine interaction constants, whereas quantitative separation of the contributions of the electric polarization and bond deformation would have required a preliminary calculation of the structure of the centers. At present we cannot determine sufficiently accurately the radial wave functions of the filled electron shells of the Gd^{3+} ion allowing for their dependence on the magnetic moment of the $4f^7$ shell and, therefore, we cannot check additionally the results obtained. It would be of considerable interest to carry out a similar investigation of the cubic rare-earth ion centers (for example, Tm^{2+} or Yb^{3+} [8]) with the predominant contribution of the covalent mechanism of the superhyperfine interaction, which can be calculated theoretically. The anomalous change in the value of $A_p - A_s$ as a result of the trigonal deformation of the $BaF_2:Tm^{2+}$ lattice, observed by Baker and Fainstein,[18] is clearly associated with the pressure-induced electrostatic polarization of the ligands, so that in the case of the ENDOR spectra of the nuclei in the ligands of the Tm^{2+} and Yb^{3+} ions in crystals with the fluorite structure we may expect relatively strong electric field effects.

[1] The values in parentheses give the corresponding parameters for the regular fluorite lattice.

[1] A. B. Roĭtsin, Usp. Fiz. Nauk 105, 677 (1971) [Sov. Phys. Usp. 14, 766 (1972)].

[2] Z. Usmani and J. F. Reichert, Phys. Rev. 180, 482 (1969).

[3] S. V. Kasatochkin and E. N. Yakovlev, Fiz. Tverd. Tela (Leningrad) 17, 520 (1975) [Sov. Phys. Solid State 17, 324 (1975)].

[4] J. M. Baker and T. Christidis, Phys. Lett. A 59, 171 (1976).

[5] J. M. Baker, J. Phys. C 1, 1670 (1968).

[6] Yu. A. Sherstkov, Yu. G. Romanov, V. A. Rybakov, and V. N. Esyunin, Uch. Zap. Ural. Gos. Univ. Ser. Fiz. No. 7, 118 (1971).

Arkhipov *et al.*

[7]J. M. Baker and T. Christidis, J. Phys. C **10**, 1059 (1977).

[8]B. R. McGarvey, J. Chem. Phys. **65**, 955 (1976).

[9]R. E. Watson and A. J. Freeman, Phys. Rev. **156**, 251 (1967).

[10]A. Abragam and B. Bleaney, Electron Paramagnetic Resonance of Transition Ions, Oxford University Press, 1970 (Russ. Transl., Mir, M., 1972-3).

[11]R. Srinivasan, Phys. Rev. **165**, 1041 (1968).

[12]P. S. Ho and A. J. Ruoff, Phys. Rev. **161**, 864 (1967).

[13]B. Z. Malkin, Paramagnitnyĭ rezonans (Paramagnetic Resonance), No. 12, Kazan University, 1976, p. 3.

[14]S. A. Arkhipov and B. Z. Malkin, Paramagnitnyĭ rezonans (Paramagnetic Resonance), No. 12, Kazan University, 1976, p. 36.

[15]N. N. Kristofel', Fiz. Tverd. Tela (Leningrad) **5**, 2367 (1963) [Sov. Phys. Solid State **5**, 1722 (1964)].

[16]Z. I. Ivanenko and B. Z. Malkin, Fiz. Tverd. Tela (Leningrad) **11**, 1859 (1969) [Sov. Phys. Solid State **11**, 1498 (1970)].

[17]M. M. Elcombe and A. W. Pryor, J. Phys. C **3**, 492 (1970).

[18]J. M. Baker and C. Fainstein, J. Phys. C **8**, 3685 (1975).

Translated by A. Tybulewicz

Alternating-current Josephson effect

G. F. Zharkov and Yu. K. Al'tudov

P. N. Lebedev Physics Institute, USSR Academy of Sciences, Moscow
(Submitted 14 October 1977)
Zh. Eksp. Teor. Fiz. **74**, 1727–1737 (May 1978)

An analysis is made of the problem of nonlinear oscillations which appear in a circuit containing a Josephson tunnel junction. The nonlinear ac equation, describing steady-state spontaneous oscillations in the circuit, is solved asymptotically. Numerical methods are used to find the dependence of the oscillation period on the circuit parameters. Hysteresis effects are studied and the range of their existence is determined. The form of the current-voltage characteristics of a Josephson circuit is considered in the case of a constant voltage supplied by an external power source.

PACS numbers: 74.50.+r

The dc Josephson effect is produced by the passage, through a Josephson tunnel junction, of a current not exceeding a certain critical value I_c.[1-4] The voltage drop across the junction is then zero, $V = 0$, and the current $I = I_c \sin\varphi$ is set up by an external voltage or current source. [The quantity $\varphi = \sin^{-1}(I/I_c)$ is known as the phase shift of the order parameter in a superconducting circuit.] If the current I exceeds I_c, the dc Josephson effect is observed: in this case a nonzero voltage drop V is established across the junction and the dependence $I(V)$ has characteristic features.[3,4]

Usually the ac Josephson effect is investigated either for a constant current I through the junction or for a constant voltage V across the junction; the majority of the experimental and theoretical investigations has been concerned specifically with these cases.[3,4] However, it is interesting to consider the problem of the ac Josephson effect in the presence of a constant external voltage U (the source of U may be a battery or a voltage generator). This case is considered in the present paper. We shall also touch upon some methodological aspects associated with the treatment of the ac Josephson effect.

We shall consider a circuit (Fig. 1) consisting of a generator of a constant voltage U, an external resistance R_0, and a tunnel junction characterized by a capacitance C and a voltage drop V. The equation for the current in the circuit is then

$$IR_0 = U - V - \frac{1}{c}\frac{\partial\Phi}{\partial t},\tag{1}$$

where Φ is the magnetic flux in the circuit, and the total current is governed by its value passing through the tunnel barrier:

$$I = I_c \sin\varphi + \frac{V}{R_t} + C\frac{dV}{dt}.\tag{2}$$

Here, the first term is the Josephson current, the second is the conduction current (R_t is the resistance to the normal component of the current through the junction), and the third is the displacement current.

We shall confine our attention to the case when there is no external magnetic field and we may assume that the current through the junction is independent of the coordinates in the junction plane (this condition is satisfied, for example, by small-area contacts). The val-
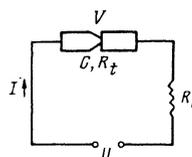

FIG. 1. Schematic diagram of a circuit with a tunnel junction.